J Therm Anal Calorim (2010) 102:1155–1160
DOI 10.1007/s10973-010-0879-5

Low-temperature heat capacities and thermodynamic properties of $Mn_3(HEDTA)_2{\cdot}10H_2O$

Cheng-Li Jiao · Li-Fang Song · Chun-Hong Jiang · Jian Zhang · Xiao-Liang Si · Shu-Jun Qiu · Shuang Wang · Li-Xian Sun · Fen Xu · Fen Li · Ji-Jun Zhao

Received: 22 February 2010 / Accepted: 6 May 2010 / Published online: 28 May 2010

Abstract The low-temperature molar heat capacity of crystalline $Mn_3(HEDTA)_2{\cdot}10H_2O$ was measured by temperature-modulated differential scanning calorimetry (TMDSC) for the first time. The thermodynamic parameters such as entropy and enthalpy relative to 298.15 K were calculated based on the above molar heat capacity data. The compound was characterized by powder XRD, FT-IR spectrum. Moreover, the thermal decomposition characteristics of $Mn_3(HEDTA)_2{\cdot}10H_2O$ were investigated by thermogravimetry–mass spectrometer (TG–MS). The experimental result through TG measurement shows that a three-step mass loss process exists. H_2O, CO_2, NO, and NO_2 were observed as products for oxidative degradation of $Mn_3(HEDTA)_2{\cdot}10H_2O$ from the MS curves.

C.-L. Jiao · L.-F. Song · C.-H. Jiang · J. Zhang · X.-L. Si · S.-J. Qiu · S. Wang · L.-X. Sun (✉) · F. Li
Materials and Thermochemistry Laboratory, Dalian Institute of Chemical Physics, Chinese Academy of Sciences, 457 Zhongshan Road, Dalian 116023, People's Republic of China
e-mail: lxsun@dicp.ac.cn

F. Xu
Faculty of Chemistry and Chemical Engineering, Liaoning Normal University, Dalian 116029, People's Republic of China

C.-L. Jiao · L.-F. Song · C.-H. Jiang · X.-L. Si · S.-J. Qiu · S. Wang
Graduate School of the Chinese Academy of Sciences, Beijing 100049, People's Republic of China

J.-J. Zhao
Laboratory of Materials Modification by Laser, Electron, and Ion Beams, Dalian University of Technology, Dalian 116024, China

Keywords EDTA · Manganese · Molar heat capacity · TG · TMDSC

Introduction

A large number of metal-EDTA compound systems have been synthesized to date [1–7]. As a multidentate ligand, depending upon reaction conditions, the reactions between a range of metal salts and EDTA salts can produce various compounds with different coordination environments, such as $(NH_4)_2[Mn(EDTA)(H_2O)]{\cdot}3H_2O$ [8], $[Mn(H_2O)_4][Mn(HEDTA)(H_2O)]_2{\cdot}4H_2O$ [9], $Ln_2Mn_3(EDTA)_3(H_2O)_{11}{\cdot}12H_2O$ (Ln = Nd, Gd) [10], $Mn_3(HEDTA)_2{\cdot}10H_2O$ [11].

These compounds are widely used in industry [12], environmental chemistry [13], catalysis [14, 15], analytically related investigations [16], and so on. However, investigations on their thermodynamic properties are scanty. Moreover, these compounds may have potential of hydrogen storage. Thus, making a detailed understanding of their thermal properties is highly desirable.

It is well known that heat capacity is one of the most fundamental thermodynamic properties of substances. Molar heat capacities of the materials at different temperatures have attracted many researchers' attention as basic data in chemistry and engineering, from which many other thermodynamic properties such as enthalpy and entropy can be calculated [17, 18]. Temperature-modulated differential scanning calorimetry (TMDSC) is one of easier and more accurate methods for determining heat capacity [19]. TMDSC was initially proposed in 1992 by Reading and co-workers [20]. TMDSC which applies a small sinusoidal modulation of temperature superimposed onto a linear underlying heating rate is a recent development for an extension to conventional DSC. Recently, this method

has been greatly developed for directly determining heat capacities for various materials isothermally and non-isothermally [17, 18, 21–23]. The structure and principle of the calorimeter have been described in detail by the references [24–26].

$Mn_3(HEDTA)_2{\cdot}10H_2O$ [11] is a three dimensional EDTA-bridged network with six- and seven- coordinate modes. To date, no further research about its thermodynamic properties was reported. In the present article, we reported the low-temperature molar heat capacities of $Mn_3(HEDTA)_2{\cdot}10H_2O$ measured by TMDSC over the temperature range from 203 to 463 K for the first time, and the thermodynamic parameters such as entropy and enthalpy were also calculated. The accuracy of TMDSC was established by comparing the measured heat capacities of standard sapphire (α-Al_2O_3) with previously reported values (NIST and NBS) [27, 28]. The thermal decomposition characteristics of this compound were investigated by TG–MS.

Experimental

All reagents were available commercially and of analytical grade without further purification prior to use, unless specifically stated elsewhere.

Sample preparation

$Mn_3(HEDTA)_2{\cdot}10H_2O$ was prepared by a previously reported procedure [11]. A mixture of H_4EDTA (0.292 g, 1 mmol) and $MnCO_3$ (0.172 g, 1.5 mmol) in 10 mL H_2O was heated with stirring until the solution was clarifying and the pH value was around 3. After 2 days, crystalline $Mn_3(HEDTA)_2{\cdot}10H_2O$ was obtained by evaporation of the resulting solution. After filtration, the product was washed with distilled water and then dried at 313 K under vacuum overnight.

Characterization

Powder X-ray diffraction pattern of the sample was collected in a X'Pert PRO X-ray diffractometer operated at 40 kV and 40 mA with a Cu Ka radiation ($\lambda = 1.5418$ nm). FT-IR spectrum was recorded on a Nicolet 380 FT-IR spectrometer using KBr pellet in the wavelength range of 4,000–400 cm^{-1}.

FT-IR (KBr pellet, 4,000–400 cm^{-1}): 3480(br), 1698(w), 1601(vs), 1446(m), 1416(s), 1344 (m), 1293(m), 1258(m), 1110(s), 1029(w), 983(m), 930(m), 855(m), 697(w), 647(w). For the sample, the absorption band located at 1,601 cm^{-1}, can be assigned to –COO asymmetric stretchings, whereas bands at 1,446 and 1,416 cm^{-1} can be assigned to –COO symmetric stretchings [29]. An additional absorption peak is observed at 1,698 cm^{-1}, which can be attributed to the protonated form (–COOH) of HEDTA.

Heat capacity measurement

Heat capacity measurements were performed on DSC Q1000 (T-zero DSC-technology, TA Instruments Inc., USA) with dry nitrogen gas with high purity (99.999%) as purge gas (50 mL min^{-1}) through the DSC cells. As described in our previous studies [30, 31], a mechanical cooling system was used for the experimental measurement and the temperature scale of the instrument was initially calibrated in the standard DSC mode, using the extrapolated onset temperatures of the melting of indium (429.75 K) at a heating rate of 10 K min^{-1}. The energy scale was calibrated with the heat of fusion of indium (28.45 J g^{-1}). The heat capacity calibration which is similar to our previous publication [31] was made by running a standard sapphire (α-Al_2O_3) at each temperature. The calibration method and the experiment were performed at the same conditions as follows: (1) sampling interval: 1.00 s/pt; (2) zero heat flow at 328.15 K; (3) equilibrate at 183.15 K; (4) isothermal for 5.00 min; (5) temperature ramp at 10 K min^{-1} to 473.15 K.

The masses of the reference and sample pans with lids were measured to within 54.25 ± 0.05 mg. Samples were crimped in non-hermetic aluminum pans with lids. Sample mass was weighed on a METTLER TOLEDO electrobalance (AB135-S, Classic) with an accuracy of (± 0.01 mg).

Thermal analysis

Thermogravimetric analysis (TG) was performed on a Cahn Thermax 500 from 310 to 923 K under dynamic conditions (100 mL min^{-1} of air) with a heating rate of 10 K min^{-1} and a sampling rate of 1 s/pt for TG curve record. The sample mass of the $Mn_3(HEDTA)_2{\cdot}10H_2O$ was 40.82 mg. The TG equipment was calibrated by the $CaC_2O_4{\cdot}H_2O$ (99.9%) with a measurement error of 3%. Mass spectra (MS) were carried out on a Multicomponent Online Gas Analyzer GAM 200.

Results and discussion

Characterization results

Powder XRD patterns for $Mn_3(HEDTA)_2{\cdot}10H_2O$ are shown in Fig. 1. The sample shows good crystallinity. The diffraction peaks of the sample prepared in this study match well with the simulated pattern according to the already published article [11], which demonstrates high

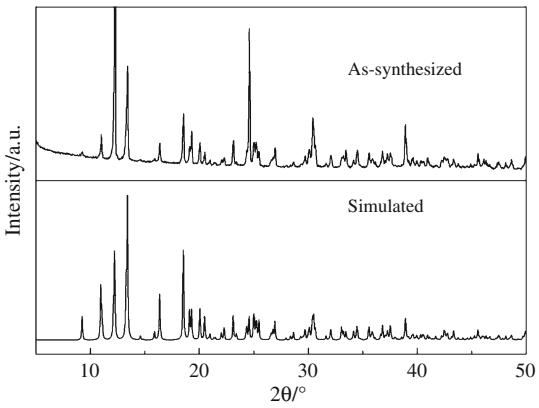

Fig. 1 X-ray diffraction patterns of $Mn_3(HEDTA)_2{\cdot}10H_2O$

purity of the compound. The program Mercury 1.4.2 was used for simulation of X-ray crystallographic powder pattern of $Mn_3(HEDTA)_2{\cdot}10H_2O$.

Heat capacity of standard sapphire (α-Al_2O_3)

Heat capacity measurements were repeated three times unless specially stated. The emphasis of this study is to assess the reproducibility and ensure accuracy of the measured data using TMDSC (Q1000). For sapphire measurement, the data of three reduplicate experiments and the experimental standard deviation for standard sapphire were collected as described in our previous study [31]. The experimental standard deviation is within ±0.0016, and the result indicates that the testing system of TMDSC is steady. Relative deviations have been calculated by the following equation:

$$\mathrm{RD}(\%) = 100\left[C_{\mathrm{p,m}}(\mathrm{exp}) - C_{\mathrm{p,m}}(\mathrm{ref})\right]/C_{\mathrm{p,m}}(\mathrm{ref}) \qquad (1)$$

where $C_{\mathrm{p,m}}$ (exp) is the experimental heat capacities and $C_{\mathrm{p,m}}$ (ref) is the referenced heat capacities. The results show that the relative deviation of our calibration data from the recommended value [27] over the whole temperature range was within ±2.2%.

Heat capacity of $Mn_3(HEDTA)_2{\cdot}10H_2O$

The heat capacities of the sample were measured by three reduplicate experiments. The experimental standard deviations below 0.024 are obtained and show reasonably good reproducibility in the temperature range from 203 to 363 K. The curves of experimental molar heat capacities of $Mn_3(HEDTA)_2{\cdot}10H_2O$ versus temperature are shown in Fig. 2.

The mean molar heat capacities of the sample are fitted to the following equation of heat capacities ($C_{\mathrm{p,m}}$) with reduced temperature (t):

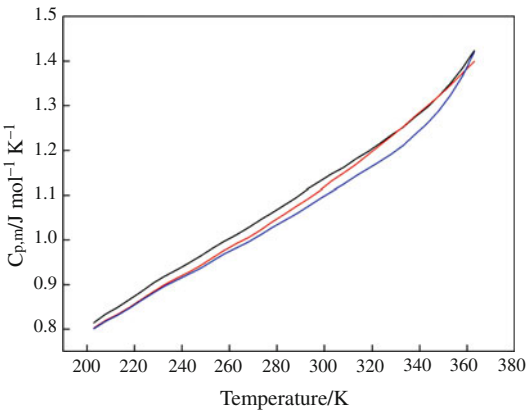

Fig. 2 The curves of experimental molar heat capacities ($C_{\mathrm{p,m}}$) vs. T for $Mn_3(HEDTA)_2{\cdot}10H_2O$

from T = (203 to 363) K,

$$C_{\mathrm{p,m}}\left[\mathrm{J\ mol^{-1}\ K^{-1}}\right] = 979.3 + 244.6t + 11.65t^2 - 10.84t^3 + 32.58t^4 + 47.34t^5 \qquad (2)$$

where $t = (T - 283)/80$ and T is the experimental temperature, 283 is obtained from polynomial $(T_{\max} + T_{\min})/2$, 80 is obtained from polynomial $(T_{\max} - T_{\min})/2$, $T_{\max}$ is the upper limit (363 K) of the above temperature region, $T_{\min}$ is the lower limit (203 K) of the above temperature region. The correlation coefficient of the fitting, $R^2 = 0.99994$. The relative deviations of all the fitting heat capacity values to the experimental points are within ±0.38%. Based on Eq. 2, the heat capacity of the sample at 298.15 K was calculated to be 1026.02 J $\mathrm{mol^{-1}\ K^{-1}}$.

From Fig. 2, it can be seen that no phase transition or thermal anomaly is observed in the experimental temperature range. This indicates that the sample is stable in this temperature region. We can also see that the heat capacity of the sample increases with increasing temperature continuously in the temperature range from 203 to 363 K.

Thermodynamic functions of $Mn_3(HEDTA)_2{\cdot}10H_2O$

Enthalpy and entropy of substances are basic thermodynamic functions relative to physical and chemical properties. In terms of the polynomials of molar heat capacity and the thermodynamic relationship, the $[H_T - H_{298.15}]$ and $[S_T - S_{298.15}]$ of $Mn_3(HEDTA)_2{\cdot}10H_2O$ are calculated with an interval of 5 K relative to the temperature of 298.15 K. The thermodynamic relationships are as follows:

$$H_T - H_{298.15} = \int_{298.15}^{T} C_{\mathrm{p,m}}\mathrm{d}T \qquad (3)$$

Table 1 The thermodynamic parameters of $Mn_3(HEDTA)_2{\cdot}10H_2O$

T/K	$C^*_{p,m}$/J K^{-1} mol^{-1}	$H_T - H_{298.15}$/kJ mol^{-1}	$S_T - S_{298.15}$/J K^{-1} mol^{-1}	T/K	$C^*_{p,m}$/J K^{-1} mol^{-1}	$H_T - H_{298.15}$/kJ mol^{-1}	$S_T - S_{298.15}$/J K^{-1} mol^{-1}
203	742.43	−74.93	−344.92	288	994.63	−10.57	−34.86
208	760.04	−72.54	−326.08	293	1010.05	−5.44	−17.66
213	776.27	−69.88	−307.04	298	1025.55	−0.16	−0.51
218	791.50	−66.99	−287.93	298.15	1026.02	0	0
223	806.05	−63.90	−268.86	303	1041.18	5.28	16.59
228	820.17	−60.65	−249.90	308	1057.00	10.88	33.67
233	834.08	−57.24	−231.09	313	1073.09	16.65	50.73
238	847.92	−53.70	−212.46	318	1089.59	22.60	67.81
243	861.82	−50.01	−194.02	323	1106.67	28.73	84.95
248	875.86	−46.20	−175.76	328	1124.57	35.07	102.18
253	890.08	−42.24	−157.69	333	1143.57	41.64	119.60
258	904.50	−38.15	−139.78	338	1164.00	48.48	137.28
263	919.13	−33.92	−122.02	343	1186.27	55.64	155.36
268	933.95	−29.55	−104.39	348	1210.88	63.17	173.99
273	948.93	−25.03	−86.87	353	1238.36	71.15	193.38
278	964.06	−20.36	−69.45	358	1269.37	79.66	213.76
283	979.30	−15.54	−52.12	363	1304.63	88.83	235.43

$C^*_{p,m}$ is calculated through Eq. 2

$$S_T - S_{298.15} = \int_{298.15}^{T} (C_{p,m}/T)dT \quad (4)$$

The values of thermodynamic function $[H_T - H_{298.15}]$ and $[S_T - S_{298.15}]$ are listed in Table 1.

Thermal stabilities and decomposition of $Mn_3(HEDTA)_2{\cdot}10H_2O$

TG analysis (Fig. 3) of $Mn_3(HEDTA)_2{\cdot}10H_2O$ shows that the three-step mass loss occurs in the temperature range of 310 to 923 K. The first mass loss starts at about 371 K and is about 19.18% (cal. 19.49%). It is in good agreement with the dehydration from $Mn_3(HEDTA)_2{\cdot}10H_2O$ to $Mn_3(HEDTA)_2$, which is confirmed by the MS curve ($m/z = 18$ and $m/z = 17$) (Fig. 4). The crystal structure collapses through the first mass loss, because nine H_2O molecules take part in coordination to Mn ion in the network. Further decomposition in the region of 456–743 K is divided into two steps in a continuous way according to the degradation of HEDTA. The second mass loss between 456 and 578 K is about 9.63% (cal. 9.75%) due to the decomposition of –COOH which did not coordinate to metal ion. The MS curve shows that the gas degradation products between 456 and 578 K are mainly CO_2

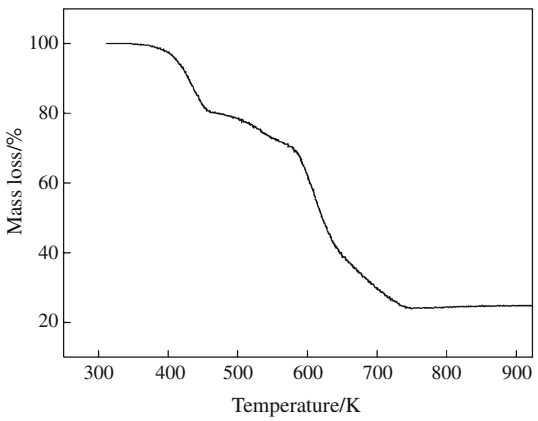

Fig. 3 TG curve of $Mn_3(HEDTA)_2{\cdot}10H_2O$

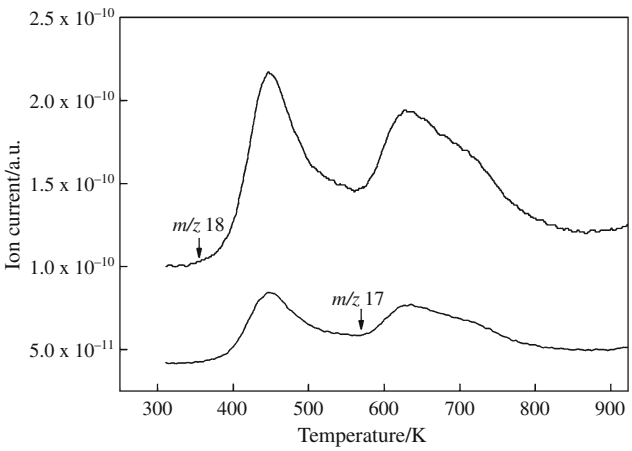

Fig. 4 MS curves of $Mn_3(HEDTA)_2{\cdot}10H_2O$: $m/z = 18$, 17

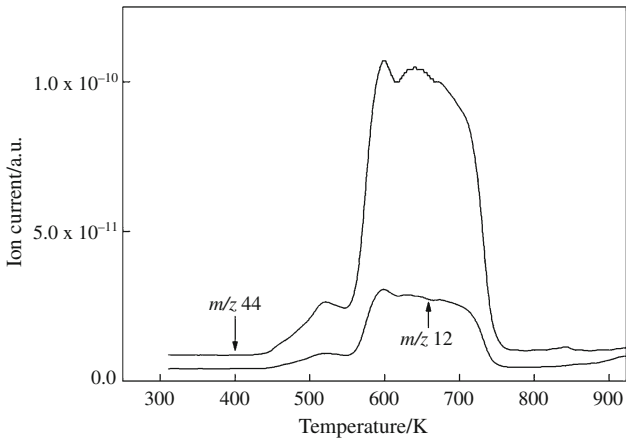

Fig. 5 MS curves of $Mn_3(HEDTA)_2{\cdot}10H_2O$: $m/z = 44$, 12

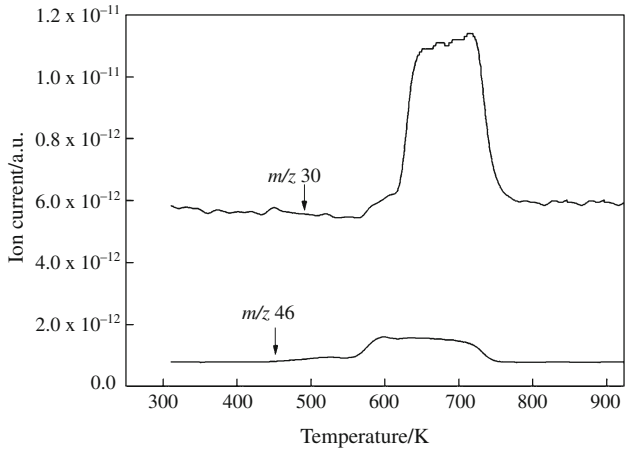

Fig. 6 MS curves of $Mn_3(HEDTA)_2{\cdot}10H_2O$: $m/z = 46$, 30

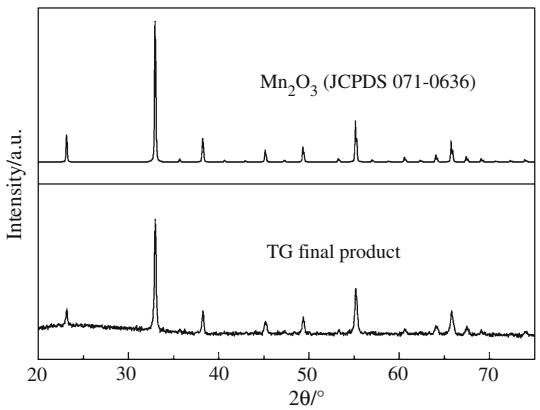

Fig. 7 X-ray diffraction patterns of TG final product and Mn_2O_3

($m/z = 44$ and $m/z = 12$) (Fig. 5) and little H_2O ($m/z = 18$ and $m/z = 17$). The third mass loss occurs in the temperature range of 578–743 K, and the corresponding gas products are mainly H_2O ($m/z = 18$ and $m/z = 17$), CO_2 ($m/z = 44$ and $m/z = 12$), NO ($m/z = 30$) and NO_2 ($m/z = 30$ and $m/z = 46$) (Fig. 6). The overall mass loss of the sample is about 75.96% (cal. 74.36%), which indicates that the sample was probably decomposed into the Mn_2O_3 as demonstrated in Fig. 7.

Conclusions

In this study, crystalline $Mn_3(HEDTA)_2{\cdot}10H_2O$ has been prepared and characterized by powder X-ray diffraction and FT-IR spectrum. The FTIR spectroscopy manifested that –COOH of H_4EDTA is not coordinated to the metal ion. The low-temperature molar heat capacities of crystal $Mn_3(HEDTA)_2{\cdot}10H_2O$ were measured by the temperature-modulated differential scanning calorimetry (TMDSC) for the first time. The heat capacity of the sample at 298.15 K was calculated to be 1023.26 J mol^{-1} K^{-1}. The thermodynamic function data relative to the reference temperature (298.15 K) were calculated based on the heat capacities measurements. Moreover, the thermal stability and decomposition mechanism of the compound was further investigated by TG–MS. The experimental results show that a three-step mass loss occurs in the temperature range of 310–923 K.

Acknowledgements The authors gratefully acknowledge the financial support for this study from the National Natural Science Foundation of China (No. 20833009, 20903095, 20873148, and U0734005) and the National Basic Research Program (973 program) of China (2010CB631303).

References

1. Zubkowski JD, Perry DL, Valente EJ, Lott S. A seven coordinate co-EDTA complex. Crystal and molecular structure of aquo(ethylenediaminetriacetatoacetic acid)cobalt(III) dihydrate. Inorg Chem. 1996;35:6352.
2. Zasurskaya LA, Polyakova IN, Poznyak AL, Polynova TN, Sergienko. Crystal structure of strontium aqua(ethylenediamine tetraacetato)cobaltate(II) tetrahydrate $Sr[CoEdta(H_2O)]{\cdot}4H_2O$. Crystallogr Rep. 2001;46:377–82.
3. Davidovich RL, Gerasimenko AV, Logvinova VB. Synthesis and crystal structure of manganese(II) ethylenediaminetetraacetatoplumbate(II) tetrahydrate. Russ J Inorg Chem. 2004;49:694–9.
4. Wang J, Wang Y, Zhang ZH, Zhang XD, Tong J, Liu XZ, et al. Syntheses, characterization, and structure determination of nine-coordinate $Na[Y\text{-}III(edta)(H_2O)_3]{\cdot}5H_2O$ and eight-coordinate $Na[Y\text{-}III(cydta)(H_2O)_2]{\cdot}5H_2O$ complexes. J Struct Chem. 2005;46:895–905.
5. Antsyshkina AS, Sadikov GG, Sergienko VS, Poznyak AL. The crystal structure of $[Mg(H_2O)_6][VO(edta)]{\cdot}3.5H_2O$. Russ J Inorg Chem. 2007;52:510–7.
6. Huang HM, Yang HB, Li XY, Ren FF. Diammonium aqua (ethylenediaminetetraacetato) iron(II) trihydrate. Acta Crystallogr Sect E Struct Rep Online. 2009;65:m87–m88.
7. Liu B, Gao J, Wang J, Wang YF, Xu R, Hu P, et al. Synthesis and structures of nine-coordinate $K[Dy(Edta)(H_2O)_3]{\cdot}3.5H_2O$, $(NH_4)_3$

[Dy(Ttha)]·5H_2O, and eight-coordinate NH_4[Dy(Cydta)(H_2O)$_2$]·4.5H_2O complexes. Russ J Coord Chem. 2009;35:422–8.
8. Wang XF, Gao J, Wang J, Zhang ZH, Wang YF, Chen LJ, et al. Crystal structures of seven-coordinate (NH_4)$_2$[Mn-II(edta)(H_2O)]·3H_2O, (NH_4)$_2$[Mn-II(cydta)(H_2O)]·4H_2O and K-2[MNII(Hdtpa)]·3.5H_2O complexes. J Struct Chem. 2008;49:724–31.
9. Polyakova IN, Poznyak AL, Sergienko VS, Stopolyanskaya LV. Crystal structures of acid ethylenediaminetetraacetates [Cd(H_2Edta)(H_2O)]·2H_2O and [Mn(H_2O)$_4$][Mn(HEdta)(H_2O)]$_2$ · 4H_2O. Crystallogr Rep. 2001;46:40–5.
10. Yi T, Gao S, Li BG. Edta-linked 4f–3d heterometallic two dimensional sheet in Ln2M3(edta)3(H_2O)11·12H_2O (Ln = Nd, Gd; M = Mn, Co). Polyhedron. 1998;17:2243–8.
11. Richards S, Pedersen B, Silverton JV, Hoard JL. Stereochemistry of ethylenediamine tetraacetato complexes. I. The structure of crystalline Mn_3(HY)10H_2O and the configuration of the seven-coordinate Mn (OH_2)Y^{-2} ion. Inorg Chem. 1964;3:27–33.
12. Judzentiene A, Jagminas A, Padarauskas A. Application of ion interaction chromatography in the electroplating industry. Chem Anal (Warsaw). 1997;42:527–34.
13. AlMasri MS, Hamwi A, Mikhlallaty H. Radiochemical determination of lead-210 in environmental water samples using Cerenkov counting. J Radioanal Nucl Chem. 1997;219:73–5.
14. Chen L, Li YQ, Huang XJ, Zhou MY. One-pot synthesis of 2-amino-2-chromenes catalyzed by tetrasodium ethylenediaminetetraacetate. Chin J Org Chem. 2009;29:437–40.
15. Bhor MD, Panda AG, Jagtap SR, Bhanage BM. Hydrogenation of alpha, beta-unsaturated carbonyl compounds using recyclable water-soluble Fe-II/EDTA complex catalyst. Catal Lett. 2008; 124:157–64.
16. Ahmed MJ, Haque ME. A rapid spectrophotometric method for the determination of molybdenum in industrial, environmental, biological and soil samples using 5, 7-dibromo-8-hydroxyquinoline. Anal Sci. 2002;18:433–9.
17. Wunderlich B. The tribulations and successes on the road from DSC to TMDSC in the 20th century the prospects for the 21st century. J Therm Anal Calorim. 2004;78(1):7–31.
18. Qi YN, Zhang J, Qiu SJ, Sun LX, Xu F, Zhu M, et al. Thermal stability, decomposition and glass transition behavior of PANI/NiO composites. J Therm Anal Calorim. 2009;98:533–7.
19. Androsch R. Heat capacity measurements using temperature-modulated heat flux DSC with close control of the heater temperature. J Therm Anal Calorim. 2000;61(1):75–89.
20. Reading M, Elliot D, Hill VL, Some aspects of the theory and practise of modulated differential scanning calorimetry. In: Proceedings of the 21st North American Thermal Analysis Society Conference, Atlanta, Georgia; 1992. p. 145–150.
21. Chau J, Garlicka I, Wolf C, Teh J. Modulated DSC as a tool for polyethylene structure characterization. J Therm Anal Calorim. 2007;90:713–9.
22. Ishida H, Rimdusit S. Heat capacity measurement of boron nitride-filled polybenzoxazine—The composite structure-insensitive property. J Therm Anal Calorim. 1999;58(3):497–507.
23. Zhang J, Zeng JL, Liu YY, Sun LX, Xu F, You WS, et al. Thermal decomposition kinetics of the synthetic complex Pb(1,4-BDC)·(DMF)(H_2O). J Therm Anal Calorim. 2008;91:189–93.
24. Wunderlich B, Jin YM, Boller A. Mathematical-description of differential scanning calorimetry based on periodic temperature modulation. Thermochim Acta. 1994;238:277–93.
25. Danley RL. New modulated DSC measurement technique. Thermochim Acta. 2003;402:91–8.
26. Wunderlich B. The contributions of MDSC to the understanding of the thermodynamics of polymers. J Therm Anal Calorim. 2006;85:179–87.
27. Archer DG. Thermodynamic properties of synthetic sapphire (Alpha-Al_2O_3), standard reference material 720 and the effect of temperature-scale differences on thermodynamic properties. J Phys Chem Ref Data. 1993;22:1441–53.
28. Ginnings DC, Furukawa GT. Heat capacity standards for the range 14°K to 1200°K. J Am Chem Soc. 1953;75:522–7.
29. Stavila V, Gulea A, Popa N, Shova S, Merbach A, Simonov YA, et al. A novel 3D Nd(III)-Bi(III) coordination polymer generated from EDTA ligand. Inorg Chem Commun. 2004;7(5):634–7.
30. Qiu SJ, Chu HL, Zhang J, Qi YN, Sun LX, Xu F. Heat capacities and thermodynamic properties of CoPc and CoTMPP. J Therm Anal Calorim. 2008;91:841–8.
31. Zhang J, Liu YY, Zeng JL, Xu F, Sun LX, You WS, et al. Thermodynamic properties and thermal stability of the synthetic zinc formate dihydrate. J Therm Anal Calorim. 2008;91:861–6.